

Phenomenological studies of top-pair production + jet at NLO

S. Dittmaier^{1,2}, P. Uwer³ and S. Weinzierl⁴

¹ *Physikalisches Institut, Universität Freiburg, D-79104 Freiburg, Germany*

² *Max-Planck-Institut für Physik (Werner-Heisenberg-Institut), D-80805 München, Germany*

³ *Institut für Physik, Humboldt-Universität zu Berlin, D-12489 Berlin, Germany*

⁴ *Institut für Physik, Universität Mainz, D-55099 Mainz, Germany*

In this talk we discuss top-quark pair production in association with an additional jet. We present numerical results based on a next-to-leading order QCD calculation.

1 Introduction

Top-quark physics is currently studied at the Tevatron and will be on the agenda of the two main LHC experiments, as soon as the LHC is turned on. The top-quark is by far the heaviest elementary fermion in the Standard Model. The large top mass is close to the scale of electroweak symmetry breaking and it is reasonable to expect that the top-quark is particularly sensitive to the details of the mechanism of electroweak symmetry breaking.

The production of a top-quark pair together with an additional jet is an important reaction. This is clear from the simple observation that a substantial number of events in the inclusive top-quark sample is accompanied by an additional jet. Depending on the energy of the additional jet the fraction of events with an additional jet can easily be of the order of 10–30% or even more. For example at the LHC we find a cross section of 376 pb for the production of a top–antitop-quark pair with an additional jet with a transverse momentum above 50 GeV. This is almost half of the total top-quark pair cross section which is 806 pb¹ if evaluated in next-to-leading order (NLO).

Ignoring the Standard Model as *the theory* of particle physics one might wonder whether the top-quark, which is almost as heavy as a gold atom, behaves as a point-like particle. A deviation from the point-like nature would appear as anomalous moments yielding differential distributions different from the point-like case. Anomalous couplings to the gluon are most naturally probed via the production of an additional jet.

The emission of an additional gluon also leads to a rather interesting property of the cross section: The differential cross section contains contributions from the interference of C-odd and C-even parts of the amplitude^{2–5}, where C denotes the charge conjugation. While for the total cross section these contributions cancel when integrating over the (symmetric) phase space they can lead to a forward–backward charge asymmetry of the top-quark which is currently measured at the Tevatron^{6,7}.

Apart from its significance as signal process it turns out that $t\bar{t}$ + jet production is also an important background to various new physics searches. A prominent example is Higgs production via vector-boson fusion. The major background to this reaction is due to $t\bar{t}$ + jet, again underlining the need for precise theoretical predictions for this process. In this talk we discuss predictions based on an NLO calculation^{8,9}.

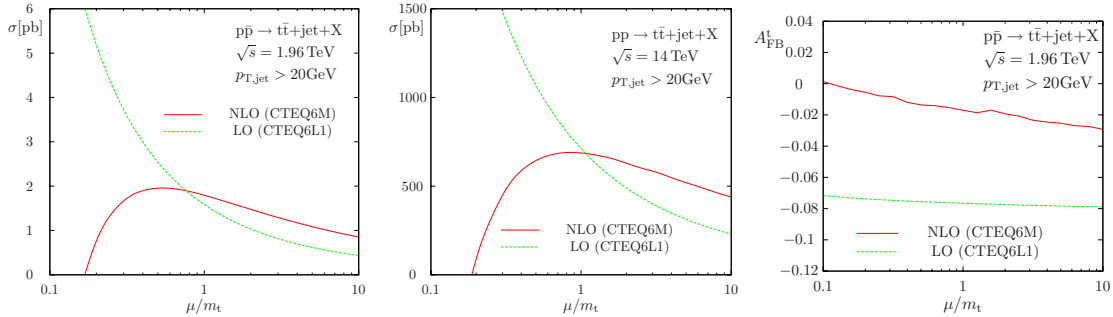


Figure 1: Scale dependence at LO (green) and NLO (red). The left plot shows the cross section for $t\bar{t}$ +jet production at the Tevatron, the middle one shows the corresponding plot for the LHC. The right plot shows the forward-backward charge asymmetry at the Tevatron.

2 The calculation

As with any NLO calculation there are real and virtual corrections. The matrix elements corresponding to the real emission contribution are given by the square of the Born amplitudes with 6 partons. All relevant matrix elements for this contribution can be obtained by crossing from the generic matrix elements

$$0 \rightarrow t\bar{t}g g g, \quad 0 \rightarrow t\bar{t}q\bar{q}g g, \quad 0 \rightarrow t\bar{t}q\bar{q}q'q', \quad 0 \rightarrow t\bar{t}q\bar{q}q\bar{q}. \quad (1)$$

The matrix elements for the virtual contribution are given by the interference term of the one-loop amplitudes with 5 partons with the corresponding Born amplitude. The required generic matrix elements are

$$0 \rightarrow t\bar{t}g g g, \quad 0 \rightarrow t\bar{t}q\bar{q}g g. \quad (2)$$

Taken individually, the real and the virtual contributions are infrared divergent. Only their sum is finite. We use the dipole subtraction formalism^{10–12} to render the individual contributions finite. The virtual one-loop diagrams consist of self-energy, vertex, box-type, and pentagon-type corrections. The most complicated diagrams are the pentagon diagrams. We use highly automated procedures for all contributions and various procedures to ensure numerical stability and efficiency^{13–24}. To ensure correctness we have for every piece two independent implementations, using where ever possible different methods and tools^{25–31}.

3 Numerical results

For the numerical analysis we use the value $m_t = 174\text{GeV}$ for the top-quark mass, CTEQ6L1 PDFs together with a one-loop running α_s in LO, as well as CTEQ6M PDFs with a two-loop running α_s in NLO. The number of active flavours is $N_F = 5$, and the respective QCD parameters are $\Lambda_5^{\text{LO}} = 165\text{MeV}$ and $\Lambda_5^{\overline{\text{MS}}} = 226\text{MeV}$. We identify the renormalisation and factorisation scales, $\mu = \mu_{\text{ren}} = \mu_{\text{fact}}$. The additional jet is defined by the Ellis-Soper k_{\perp} -jet algorithm³² with $R = 1$ and we require a transverse momentum of $p_{T,\text{jet}} > p_{T,\text{jet,cut}}$. For the Tevatron we use $p_{T,\text{jet,cut}} = 20\text{GeV}$, for the LHC we either use $p_{T,\text{jet,cut}} = 20\text{GeV}$ or $p_{T,\text{jet,cut}} = 50\text{GeV}$. Fig. 1 shows the scale dependence of the cross section at LO and NLO for the Tevatron and the LHC. The NLO corrections reduce the scale dependence significantly. In addition we show in Fig. 1 the forward-backward charge asymmetry at the Tevatron. In LO the asymmetry is defined by

$$A_{\text{FB,LO}}^t = \frac{\sigma_{\text{LO}}^-}{\sigma_{\text{LO}}^+}, \quad \sigma_{\text{LO}}^{\pm} = \sigma_{\text{LO}}(y_t > 0) \pm \sigma_{\text{LO}}(y_t < 0), \quad (3)$$

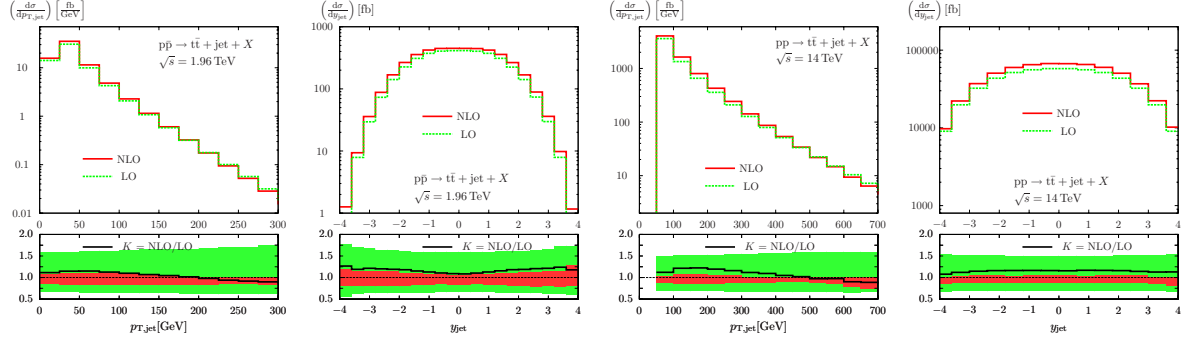


Figure 2: The distribution of the additional jet in p_T and rapidity at the Tevatron (left) and the LHC (right). The large plots show the predictions at LO (green) and NLO (red). The lower panels show the scale uncertainties, the LO scale uncertainty is shown by a green band, the NLO scale uncertainty by a red band. In addition the ratios $K = \text{NLO}/\text{LO}$ are shown by a black line.

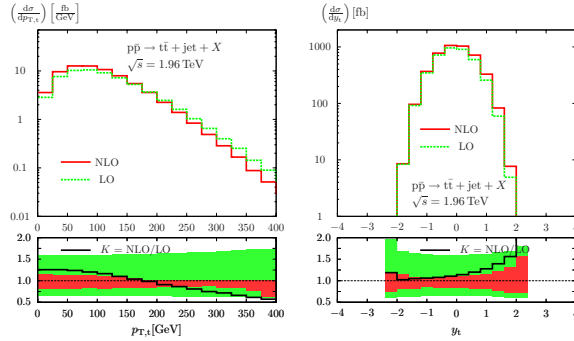


Figure 3: The distribution of the top-quark in p_T (left) and rapidity (right) at the Tevatron.

where y_t denotes the rapidity of the top-quark. Denoting the corresponding NLO contributions to the cross sections by $\delta\sigma_{\text{NLO}}^\pm$, we define the asymmetry at NLO by

$$A_{\text{FB,NLO}}^t = \frac{\sigma_{\text{LO}}^-}{\sigma_{\text{LO}}^+} \left(1 + \frac{\delta\sigma_{\text{NLO}}^-}{\sigma_{\text{LO}}^-} - \frac{\delta\sigma_{\text{NLO}}^+}{\sigma_{\text{LO}}^+} \right), \quad (4)$$

i.e. via a consistent expansion in α_s . At LO we find an asymmetry of about -8% . The scale dependence is rather small. This is a consequence of the fact that α_s cancels exactly between the numerator and the denominator. In addition the residual factorisation scale dependence also cancels to a large extent in the ratio. The NLO corrections to the asymmetry are of order α_s^1 and depend on the renormalisation scale. It is therefore natural to expect a stronger scale dependence of the asymmetry at NLO than at LO, as seen in the plot. Within the current numerical set-up the asymmetry is almost washed out at NLO.

In Fig. 2 we show the distribution of the additional jet in p_T and rapidity at the Tevatron and the LHC. In these plots we used $p_{T,\text{jet,cut}} = 20\text{GeV}$ for the Tevatron and $p_{T,\text{jet,cut}} = 50\text{GeV}$ for the LHC. The scale variations in the lower panel correspond to a variation by a factor of 2 around $\mu = m_t$. As expected, the scale uncertainties are reduced by the inclusion of the NLO corrections. Also shown in the lower panel of Fig. 2 is the ratio $K = \text{NLO}/\text{LO}$.

Finally, Fig. 3 shows the distribution of the top-quark in p_T and rapidity at the Tevatron. We note that the NLO corrections do not simply rescale the LO shape, but induce distortions of the distributions, as can be seen from the non-constant K -factor.

4 Conclusions

In this talk we discussed predictions for $t\bar{t}$ +jet production at hadron colliders based on a NLO QCD calculation. For the cross section the NLO corrections reduce significantly the scale dependence of the LO predictions. The charge asymmetry of the top-quarks at the Tevatron is significantly decreased at NLO and is almost washed out in particular when the residual scale dependence is taken into account. Further refinements of the precise definition of the forward-backward asymmetry are required to stabilise the asymmetry with respect to higher-order corrections. From a technical perspective the calculation we reported on represents a corner-stone for NLO multi-leg computations, which are required for the LHC.

References

1. S. Moch and P. Uwer, Phys. Rev. **D78**, 034003 (2008), arXiv:0804.1476.
2. F. Halzen, P. Hoyer, and C. S. Kim, Phys. Lett. **B195**, 74 (1987).
3. J. H. Kühn and G. Rodrigo, Phys. Rev. **D59**, 054017 (1999), hep-ph/9807420.
4. J. H. Kühn and G. Rodrigo, Phys. Rev. Lett. **81**, 49 (1998), hep-ph/9802268.
5. M. T. Bowen, S. D. Ellis, and D. Rainwater, Phys. Rev. **D73**, 014008 (2006), hep-ph/0509267.
6. D0, V. M. Abazov *et al.*, Phys. Rev. Lett. **100**, 142002 (2008), arXiv:0712.0851.
7. CDF, T. Aaltonen *et al.*, Phys. Rev. Lett. **101**, 202001 (2008), arXiv:0806.2472.
8. S. Dittmaier, P. Uwer, and S. Weinzierl, Phys. Rev. Lett. **98**, 262002 (2007), hep-ph/0703120.
9. S. Dittmaier, P. Uwer, and S. Weinzierl, Eur. Phys. J. **C59**, 625 (2009), arXiv:0810.0452.
10. S. Catani and M. H. Seymour, Nucl. Phys. **B485**, 291 (1997), hep-ph/9605323.
11. L. Phaf and S. Weinzierl, JHEP **04**, 006 (2001), hep-ph/0102207.
12. S. Catani, S. Dittmaier, M. H. Seymour, and Z. Trocsanyi, Nucl. Phys. **B627**, 189 (2002), hep-ph/0201036.
13. W. Beenakker and A. Denner, Nucl. Phys. **B338**, 349 (1990).
14. A. Denner, U. Nierste, and R. Scharf, Nucl. Phys. **B367**, 637 (1991).
15. W. Beenakker *et al.*, Nucl. Phys. **B653**, 151 (2003), hep-ph/0211352.
16. A. Denner and S. Dittmaier, Nucl. Phys. **B658**, 175 (2003), hep-ph/0212259.
17. S. Dittmaier, Nucl. Phys. **B675**, 447 (2003), hep-ph/0308246.
18. A. Denner and S. Dittmaier, Nucl. Phys. **B734**, 62 (2006), hep-ph/0509141.
19. A. Bredenstein, A. Denner, S. Dittmaier, and S. Pozzorini, JHEP **08**, 108 (2008), arXiv:0807.1248.
20. W. T. Giele and E. W. N. Glover, JHEP **04**, 029 (2004), hep-ph/0402152.
21. W. Giele, E. W. N. Glover, and G. Zanderighi, Nucl. Phys. Proc. Suppl. **135**, 275 (2004), hep-ph/0407016.
22. F. A. Berends and W. T. Giele, Nucl. Phys. **B306**, 759 (1988).
23. S. Weinzierl, Eur. Phys. J. **C45**, 745 (2006), hep-ph/0510157.
24. S. Weinzierl and D. A. Kosower, Phys. Rev. **D60**, 054028 (1999), hep-ph/9901277.
25. J. Küblbeck, M. Böhm, and A. Denner, Comput. Phys. Commun. **60**, 165 (1990).
26. T. Hahn, Comput. Phys. Commun. **140**, 418 (2001), hep-ph/0012260.
27. P. Nogueira, J. Comput. Phys. **105**, 279 (1993).
28. J. A. M. Vermaseren, (2000), math-ph/0010025.
29. G. J. van Oldenborgh and J. A. M. Vermaseren, Z. Phys. **C46**, 425 (1990).
30. G. J. van Oldenborgh, Comput. Phys. Commun. **66**, 1 (1991).
31. T. Stelzer and W. F. Long, Comput. Phys. Commun. **81**, 357 (1994), hep-ph/9401258.
32. S. D. Ellis and D. E. Soper, Phys. Rev. **D48**, 3160 (1993), hep-ph/9305266.